

**Universitat de Lleida**

Document downloaded from:

<http://hdl.handle.net/10459.1/65011>

The final publication is available at:

<https://doi.org/10.1016/j.aca.2016.03.035>

Copyright

cc-by-nc-nd, (c) Elsevier, 2016



Està subjecte a una llicència de [Reconeixement-NoComercial-SenseObraDerivada 4.0 de Creative Commons](https://creativecommons.org/licenses/by-nc-nd/4.0/)

1           **AGNES at vibrated gold microwire electrode for the direct**  
2           **quantification of free copper concentrations**

3  
4 Rute F. Domingos<sup>1,2,\*</sup>, Sara Carreira<sup>1</sup>, Josep Galceran<sup>3</sup>, Pascal Salaün<sup>4</sup>, José P. Pinheiro<sup>5</sup>

5  
6 <sup>1</sup> Centro de Química Estrutural, Instituto Superior Técnico, Universidade de Lisboa, Torre  
7 Sul lab 11-6.3, Av. Rovisco Pais # 1, 1049-001 Lisbon, Portugal

8 <sup>2</sup> Institut de Physique du Globe de Paris, Sorbonne Paris Cité, Université Paris Diderot,  
9 UMR CNRS 7154, 75205 Paris Cedex 05, France (Present address)

10 <sup>3</sup> Department of Chemistry, University of Lleida and Agrotecnio, Rovira Roure 191,  
11 25198 Lleida, Spain

12 <sup>4</sup> School of Environmental Sciences, University of Liverpool, 4 Brownlow Street,  
13 Liverpool L693 GP, United Kingdom

14 <sup>5</sup> LIEC/ENSG, UMR 7360 CNRS – Université de Lorraine, 15 Avenue du Charmois,  
15 54500 Vandoeuvre-les-Nancy, France

16  
17  
18  
19  
20 \*Corresponding author

21 email: [rdomingos@ipgp.fr](mailto:rdomingos@ipgp.fr)

22 phone number: (+33) 01 83 95 74 43

23  
24  
25  
26

27 **Abstract**

28 The free metal ion concentration and the dynamic features of the metal species are  
29 recognized as key to predict metal bioavailability and toxicity to aquatic organisms.  
30 Quantification of the former is, however, still challenging. In this paper, it is shown for  
31 the first time that the concentration of free copper ( $\text{Cu}^{2+}$ ) can be quantified by applying  
32 AGNES (Absence of Gradients and Nernstian equilibrium stripping) at a solid gold  
33 electrode. It was found that: i) the amount of deposited Cu follows a Nernstian  
34 relationship with the applied deposition potential, and ii) the stripping signal is linearly  
35 related with the free metal ion concentration. The performance of AGNES at the vibrating  
36 gold microwire electrode (VGME) was assessed for two labile systems: Cu-malonic acid  
37 and Cu-iminodiacetic acid at ionic strength 0.01 M and a range of pH values from 4.0 to  
38 6.0. The free Cu concentrations and conditional stability constants obtained by AGNES  
39 were in good agreement with stripping scanned voltammetry and thermodynamic  
40 theoretical predictions obtained by Visual Minteq. This work highlights the suitability of  
41 gold electrodes for the quantification of free metal ion concentrations by AGNES. It also  
42 strongly suggests that other solid electrodes may be well appropriate for such task. This  
43 new application of AGNES is a first step towards a range of applications for a number of  
44 metals in speciation, toxicological and environmental studies for the direct determination  
45 of the key parameter that is the free metal ion concentration.

46

47

48

49

50 **Keywords:** gold electrode, VGME, copper, speciation, AGNES, stripping scanned  
51 voltammetry

52

53

54 **1. Introduction**

55 When entering in a natural aquatic environment, trace metals are rapidly complexed by  
56 biotic and abiotic ligands, thus modifying their speciation and their bioavailability. The  
57 understanding and prediction of their ecotoxicological impact is dependent on our ability  
58 to measure the most relevant fractions of the trace metals in terms of bioavailability, i.e.,  
59 the free and labile metal ion concentrations.

60 The critical importance ascribed to the free ion in models, such as the free-ion activity  
61 model (FIAM) and the biotic ligand model (BLM) [1], has led to an increasing interest in  
62 quantifying these species in environmentally relevant media. However, there is only a  
63 limited number of techniques able to quantify the free ion concentration with the required  
64 selectivity and detection limit. These include potentiometry with ion-selective electrodes  
65 (ISEs) [2], the Donnan membrane technique (DMT) [3], the permeable liquid membrane  
66 (PLM) [4, 5], the ion-exchange technique (IET) [6], and the absence of gradients and  
67 Nernstian equilibrium stripping technique (AGNES) [7]. Reviews of these (and other)  
68 techniques are available [8-10]. Although all these techniques have the ability to measure  
69 the free metal ion concentration, each of them has its own limitations. For instance, the  
70 main drawback of commercial ISE is its restricted use to the quantification of proton and  
71 those elements present in total concentrations above  $10^{-6}$  M due to the solubilization and  
72 contamination/adsorption of the electrode membrane. In the last decades potentiometric  
73 sensors using polymeric membranes and special inner solutions were developed  
74 increasing the ISE's detection limit ( $10^{-10}$ - $10^{-13}$  M), however, their operation is still  
75 difficult and most are not commercially available [11, 12]. DMT performs simultaneous  
76 measurements of several elements at very low detection limit (dependent on the analytical  
77 technique used to quantify the metal content; e.g.,  $10^{-11}$ - $10^{-12}$  M by using inductively  
78 coupled plasma mass spectrometry), but the equilibration time is very long, often 24 or

79 48 h. PLM is a dynamic technique where the speciation answer depends on the rate-  
80 limiting step; the free metal ion can be measured when the diffusion across the membrane  
81 is governing the flux. However, despite the multielement quantification at the  $10^{-11}$ - $10^{-12}$   
82 M level (also dependent on the analytical technique used for the elemental analysis) when  
83 using PLM, there is a high risk of measurement of lipophilic metal complexes together  
84 with the free ions. The detection limits in IET are directly related with the quantity (and  
85 binding capacity) of the resin ( $10^{-9}$ - $10^{-6}$  M) and in some systems the equilibration times  
86 might be long. Moreover, positive interferences do occur in the presence of complex  
87 amino acid ligands.

88 AGNES, which has been increasingly used in the past decade, has been suggested as a  
89 free metal ion quantification technique overcoming most of the limitations shown by the  
90 above described techniques [13-16]. This electroanalytical technique was specifically  
91 designed at a Hg electrode to quantify low free metal ion concentrations (as low as  $10^{-10}$   
92 M), via two stages: i) deposition, where a potential  $E_1$  is applied to preconcentrate the  
93 metal inside the working electrode until the redox couple reaches Nernstian equilibrium  
94 (i.e., until there are no concentration gradients of reduced or oxidized metal); ii) stripping,  
95 where the concentration of the reduced metal is quantified. The analytical signal is the  
96 response taken from the electrochemical technique used in the stripping stage. One clear  
97 advantage of AGNES is its predictable Nernstian response, similar to an ISE, since a  
98 suitable analytical signal is linearly related with the free metal ion concentration with a  
99 proportionality factor obtained from the calibration. However, two main disadvantages  
100 need to be pointed out: i) AGNES typical implementation can only quantify free ion  
101 concentrations of metal ions that can amalgamate reversibly on a Hg electrode, and ii) the  
102 time involved in the preconcentration stage to reach equilibrium can vary from minutes  
103 to hours, although much shorter than when using techniques such as DMT or even IET.  
104 AGNES had been originally applied only at mercury electrodes, with these arising

105 concerns due to Hg toxicity and not ideal for Cu quantifications due to the proximity of  
106 their reduction potentials (see [17] and references therein). Recently, AGNES was  
107 successfully implemented at bismuth film electrodes, highlighting the possibility of  
108 applying AGNES at other solid electrode materials [18]. Unfortunately, copper speciation  
109 is not possible at Bi electrodes due to the similarity of their reduction potentials.  
110 Contrarily, gold electrodes are well suited for Cu speciation [19-22], without the need for  
111 oxygen removal, since the metal reduction wave is at more positive potentials than the O<sub>2</sub>  
112 wave [19]. Evidently, this is a significant advantage in analysis of environmental samples,  
113 since both CO<sub>2</sub> and pH are maintained in the sample, avoiding changes in metal speciation  
114 [23]. Another advantage is that the gold electrodes can be used as such, without an  
115 electrodeposited film (like for thin film Hg [24], Bi [18] and Sb [25] electrodes), which  
116 could become an issue over long measuring time periods.

117 Traditionally, gold electrodes are not widely employed in environmental samples since  
118 they can be easily contaminated and their detection limit is not sufficiently low. Recently,  
119 a vibrating gold microwire electrode (VGME) was proposed [20], and appears to be an  
120 optimal candidate for the Cu quantification in natural samples due to its high sensitivity.  
121 These gold electrodes have already been shown to successfully quantify i) total metal  
122 concentrations of various metals, including Cu [19], and ii) the conditional complex  
123 stability of inert metal complexes by scanned stripping voltammetry (SSV) [21]. The  
124 electrode vibrations offer additional advantages over other common electrode setups: i)  
125 they eliminate the need for external stirring of the solution, thus also simplifying the *in*  
126 *situ* detection in the environment [20], ii) they produce much more stable hydrodynamic  
127 conditions at the surface of the electrode leading to better reproducibility and, thus, lower  
128 detection limits [26, 27], iii) they produce a significantly higher flux of species towards  
129 the electrode due to a smaller diffusion layer, again decreasing detection limits [26], and

130 iv) the stripping can start immediately after stopping the vibration, without any  
131 equilibrium time.

132 AGNES theoretical framework was recently developed for solid electrodes [18]. The key  
133 requirement for AGNES is the attainment -by the end of the deposition stage- of Nernstian  
134 equilibrium involving the activity of the free metal ion in solution and that of the reduced  
135 metal. The AGNES principle offers the possibility to choose the activities ratio (which,  
136 in an amalgam, is proportional to the concentrations ratio or gain) just by changing the  
137 deposition potential. When  $M^0$  deposits on a solid electrode as a bulk solid phase (i.e.,  
138 when depositing a metal on its own substrate), its activity is always unity regardless of  
139 the metal amount deposited and in that case, AGNES cannot be applied. Fortunately, the  
140 activity of the reduced metal can be changed by varying the coverage of adsorbed atoms  
141 on the foreign solid surface, leading to the possibility of performing AGNES also at solid  
142 electrodes in conditions of sub-monolayer coverage [18].

143 The aim of this work is to develop and test an optimal electrochemical methodology based  
144 on AGNES principles for the direct determination of the free metal ion concentration at  
145 the solid gold electrode. The system was tested in the presence of ligands forming labile  
146 Cu complexes and results (free metal ion concentrations and conditional stability  
147 constants) were compared with speciation modeling predictions (Visual Minteq).  
148 Additional validation was obtained by comparison between the performances of AGNES  
149 and scanned stripping voltammetry (SSV).

150

## 151 **2. Experimental setting**

### 152 *2.1. Reagents and solutions*

153 All solutions were prepared in ultrapure water from a MilliQ Integral 3 (resistivity > 18  
154 M $\Omega$  cm). The Cu stock solutions were prepared by dilution of its standard solution (1000  
155 mg L<sup>-1</sup> Fluka), and the NaNO<sub>3</sub> used to adjust the ionic strength solution was prepared

156 from the solid (Merck, suprapur). HCl (Merck, suprapur) and H<sub>2</sub>SO<sub>4</sub> (Panreac), NaCl  
157 (Merck, 99.6 %), potassium hexacyanoferrate (III) (K<sub>3</sub>[Fe(CN)<sub>6</sub>]; Merck, p.a. 99 %), and  
158 KCl (Merck, p.a., 99.5%) were used for the preparation and characterization of the  
159 VGME. Malonic acid (MAL) and iminodiacetic acid (IDA) were purchased from Sigma-  
160 Aldrich (ReagentPlus 99 and 98%, respectively). HNO<sub>3</sub> (Merck, suprapur) and NaOH  
161 (Merck, p.a.) solutions were used to adjust the pH, which was measured using a Denver  
162 Instrument (model 15) and a Radiometer analytical combined pH electrode.

163

## 164 *2.2 Instrumentation, electrode preparation and maintenance*

165 Voltammetric experiments were performed using an Eco Chemie  $\mu$ Autolab III  
166 potentiostat in conjunction with a Metrohm 663VA stand and a personal computer using  
167 the GPES 4.9 software (Eco Chemie). Electrodes included a calomel reference electrode  
168 with a 0.1 M NaNO<sub>3</sub> salt bridge, a platinum counter electrode, and the VGME as the  
169 working electrode. The measurements were carried out at room temperature (20-23 °C).  
170 The gold microwire (99.99%, hard, Goodfellow, diameter ( $d$ ) = 25  $\mu$ m) was heat-sealed  
171 in a 200  $\mu$ L polypropylene pipette tip together with a copper wire (to make contact with  
172 the working electrode cable) that was previously dipped in a conductive silver solution  
173 (Leitsiber L100; that is used as a conductive adhesive), and this tip was then fitted onto a  
174 1 mL polypropylene pipet tip, which had a vibrator incorporated [20, 28]. The vibrator  
175 was driven by a 1.5 V power supply (home-built converter of 5 to 1.5 V), which was  
176 interfaced to, and powered by, the IME (Autolab, Metrohm, Switzerland), and controlled  
177 by the stirrer on/off trigger in the software (GPES, Autolab). The surface of the VGME  
178 was cleaned electrochemically by hydrogen generation at -2 V for 60 s in 0.5 M H<sub>2</sub>SO<sub>4</sub>  
179 and its behavior was checked by running 5 cyclic voltammetry scans between 0 and 1.5  
180 V (0.1 V s<sup>-1</sup>) until the response was stable, which was usually from the second scan  
181 onwards [19]. The thickness of the diffusion layer ( $\delta$ ) of the microwire electrode was

182 determined as described previously [19]. Briefly, an oxide monolayer was first formed  
183 by running (at  $100 \text{ mV s}^{-1}$ ) a cyclic voltammogram between 0 and 1.5 V in 0.5 M  $\text{H}_2\text{SO}_4$   
184 and its reduction charge used to calculate the total area, assuming a  $450 \text{ } \mu\text{C cm}^{-2}$  charge  
185 density for an oxide monolayer. The length was calculated from the chronoamperometric  
186 current obtained in a solution of 0.01 M  $\text{K}_3[\text{Fe}(\text{CN})_6]$  (prepared in 0.5 M KCl) at -0.3 V  
187 during 15 s (at a sampling frequency of  $0.01 \text{ s}^{-1}$ ) assuming a constant diameter of 25  $\mu\text{m}$   
188 (commercial specification). The  $\delta$  was calculated from the diffusion-limited current  
189 obtained under vibrated conditions.

190

### 191 *2.3 Measuring procedure*

192 Contrary to the Hg drop electrode where a new surface is produced for each single  
193 measurement, an electrochemical procedure must be used to ensure a reproducible surface  
194 of the solid electrode (in terms of adsorbed species) before each measurement. This was  
195 done here by applying at least 5 times (until the analytical signal of interest is undistorted  
196 and shoulderless) a desorption step including two consecutive potentials in the same  
197 solution as that being measured:  $E = -2 \text{ V}$  during 15 s and  $E = 0.550 \text{ V}$  during 5 s. A  
198 similar cleaning procedure of the electrode between measurements was also required for  
199 optimum stability in seawater [29]. However, in presence of ligands, a more efficient  
200 cleaning procedure was necessary; after each measurement 5 cyclic voltammetry scans  
201 between 0 and 1.5 V ( $100 \text{ mV s}^{-1}$ ) in a solution of  $\text{HNO}_3$  0.02 M were performed.

202 Each AGNES measurement consisted in the application of a deposition potential,  $E_1$ , for  
203 a specific time ( $t_1$ ) followed by a desorption pulse ( $E = -2 \text{ V}$ ,  $t = 1 \text{ s}$ ), limiting the  
204 adsorption of species that can interfere with the stripping peak, and, thus, contributing for  
205 a reproducible gold surface. This desorption pulse must be applied after each 30 s of  
206 deposition, to avoid build-up of adsorbed species leading to a continuously changing of  
207 the gold surface, and thus irreproducible replicates. For depositing times larger than 30 s,

208 sequential procedures of 30 s deposition at  $E_1$  followed by the desorption pulse were  
209 applied while keeping a standby potential ( $E_{\text{standby}} = E_1$ ) between them (i.e., the total  
210 number of sequential deposition procedures times 30 s equals the total deposition time).  
211 Such sequential procedure was previously found to significantly increase the linear range  
212 of Sb(III) at the gold electrode in similar electrolyte conditions, presumably by limiting  
213 the building-up of adsorbed acetate anions at the gold surface [30]. Because only mobile  
214 and labile complexes are tackled here, differential pulse with anodic stripping  
215 voltammetry (DPASV) was used in this work for the stripping stage. A background scan  
216 was made after each analytical scan consisting of the desorption pulse (-2 V for 1 s)  
217 followed by the same stripping as for the analytical scan, and was subtracted from the  
218 analytical scan allowing the removal of this pulse (indeed negligible compared with the  
219 main signal) from the analytical signal. The background scan was kept the same,  
220 irrespective of the deposition time and thus, irrespective of the number of desorption  
221 pulses that were applied during the deposition step. The metal reoxidation was performed  
222 by using a scan rate of  $0.040 \text{ V s}^{-1}$  and modulation amplitude of 0.025 V, modulation time  
223 of 0.008 s, and interval time 0.1 s. The derivative (i.e., the sum of the two highest  
224 derivative values corresponding to the inflection points of the peaks) of the background-  
225 corrected peak signal was used for quantification.

226

#### 227 *2.4 Cu deposition on gold*

228 The nature of Cu deposition on gold was evaluated by applying a stepwise DPASV, i.e.,  
229 a DP stripping scanned voltammetry (SSV). A forward and backward SSV were  
230 performed by doing scans from 0.000 to 0.300 V and from 0.300 to 0.000 V, respectively,  
231 with a deposition time of 30 s. The SSV waves were performed with  $1.0 \times 10^{-7} \text{ M}$  of Cu at  
232 pH 4 and  $I = 0.01 \text{ M}$ .

233

## 234 2.5 AGNES at the VGME

### 235 2.5.1 Effect of deposition potential and deposition time

236 The possibility of applying AGNES by using a VGME was first evaluated by performing  
237 the so-called “trajectory” studies where the peak intensity is measured as a function of  
238 deposition time and this is repeated at various deposition potentials. These studies  
239 together with linearity evaluation were obtained in 0.01 M NaNO<sub>3</sub> solutions adjusted at  
240 pH 4 with HNO<sub>3</sub>.

241 Trajectories (i.e., time profiles) were determined by applying a set of deposition potentials  
242 (0.185, 0.200, 0.205, 0.215, 0.230 and 0.250 V) for sufficiently long deposition times  
243 (450 to 1200 s) until the attainment of the equilibrium. A set of  $E_1$  and  $t_1$  that were found  
244 sufficient to attain AGNES conditions ( $E_1 = 0.230$  V and  $t_1 = 240$  s) were chosen for the  
245 evaluation of the linearity between the stripping signal and the free metal ion  
246 concentration ( $c_{\text{Cu,free}} = 4.9 \times 10^{-9}$  to  $4.9 \times 10^{-6}$  M).

247

### 248 2.5.2 Complexation studies of Cu-MAL and Cu-IDA

249 AGNES measurements were carried out by applying an  $E_1 = 0.230$  V and  $t_1 = 240$  s in 20  
250 mL of 0.01 M NaNO<sub>3</sub> solutions. The calibration plot included Cu concentrations from  
251  $5.0 \times 10^{-9}$  to  $1.0 \times 10^{-7}$  M measured at pH 4 designed to avoid Cu losses by adsorption onto  
252 the polystyrene container walls. Solutions of the MAL and IDA were prepared by dilution  
253 of the stock solution (prepared from the solids) into the prepared electrolyte solution  
254 (Milli-Q water with adjusted pH and ionic strength) to give the desired final  
255 concentrations of  $1.0 \times 10^{-5}$  and  $1.0 \times 10^{-4}$  M for the MAL and  $1.0 \times 10^{-6}$  and  $1.0 \times 10^{-5}$  M for  
256 IDA. Samples were prepared using a range of solution conditions: pH 4.0-6.0 for  
257 solutions containing MAL and pH 4.0-5.5 for IDA, ionic strength ( $I$ ) 0.01 M, and Cu  
258 concentration of  $1 \times 10^{-7}$  M added as metal salt.

259 The results are the mean and standard deviation of at least three replicates, performed on  
260 different days using freshly prepared samples.

261

### 262 *2.6 Scanned Stripping Voltammetry (SSV)*

263 The conditional stability constants of the formed metal complexes was evaluated by  
264 performing DP SSV [21, 27] from 0.000 to 0.300 V with a  $t_d = 30$  s (scan rate of 0.080 V  
265  $s^{-1}$  and modulation amplitude of 0.05 V, modulation time of 0.004 s, and interval time 0.1  
266 s). The same desorption step and pulse as explained in section 2.3 was applied as well as  
267 the background scan subtraction. The calibration plot was performed with  $1.0 \times 10^{-7}$  M of  
268 Cu at pH 4 and  $I = 0.01$  M ( $\text{NaNO}_3$ ). Samples were prepared using a range of solution  
269 conditions:  $c_{\text{Cu,T}} = 1.0 \times 10^{-7}$  M,  $c_{\text{MAL,T}} = 1.0 \times 10^{-5}$  M,  $c_{\text{IDA,T}} = 1.0 \times 10^{-5}$  M, pH 4.5-6.0,  $I =$   
270 0.01 M.

271 The results are the mean, minimum and maximum of at least three replicates, performed  
272 on different days using freshly prepared samples. The indicated error arises from that of  
273 the analytical signal (5 %) together with that propagated from the  $\pm 2$  mV uncertainty  
274 in the half-wave deposition potential (estimated error of the reference electrode on  
275 different days).

276

## 277 **3. Results**

### 278 *3.1 The nature of Cu deposition on gold*

279 The electrodeposition of metals at solid electrodes proceeds via (i) the formation of a  
280 monolayer of reduced metal onto the electrode, the so-called underpotential deposition  
281 (UPD), followed by (ii) the formation of new layers of metal atoms on top of previously  
282 deposited metal, which is called the bulk metal deposition that occurs at a less positive  
283 potential [31]. Thus, at a solid electrode, two (or more) reduction and stripping processes  
284 can occur, which may result in a complex interpretation of the analytical signal. Under

285 the conditions used here (0.01 M NaNO<sub>3</sub> and up to 1.0×10<sup>-7</sup> M of total Cu), only UPD  
286 occurs with the stripping potential of the copper monolayer from the gold surface  
287 occurring at *ca.* 0.275 V *vs.* SCE (Figure 1). This value is in accordance with previous  
288 studies where the stripping potential of the UPD peak was found at 0.255-0.305 V *vs.*  
289 SCE, while the stripping peak of the bulk deposition occurred at much less positive  
290 potentials, 0.005-0.105 V *vs.* SCE [31-33].

291

292 The influence of the deposition potential on the UPD signal in a non-complexing medium  
293 was evaluated by sequential SSV performed from 0.000 to 0.300 V (forward wave) and  
294 from 0.300 to 0.000 V (backward wave). Half-wave deposition potentials ( $E_{d,1/2}$ ) values  
295 were 0.218 and 0.219 V for the forward and backward scans, respectively (Figure 2). A  
296 reasonable fit between the sequential waves was obtained indicating that the cleaning  
297 procedure that is applied between each measurement is efficient.

298

### 299 *3.2 Implementation of AGNES using the VGME*

300 There are two stringent requirements for AGNES to be successfully implemented: i) at  
301 any selected  $E_1$ , the equilibrium must be attained for sufficiently long deposition times  $t_1$ ,  
302 and ii) there must be a fixed (preferably linear) relationship between the stripping signal  
303 and the free metal ion concentration (for the chosen set of  $E_1$  and  $t_1$ ).

304 A third check performed here, though not a strict requirement for the application of  
305 AGNES, is the Nernstian behavior of the measured signal with the applied potential (i.e.,  
306 the linearity between obtained signal and applied gain, see next section).

307

#### 308 3.2.1 Trajectories

309 The possibility of performing AGNES with the VGME is strictly related with the  
310 possibility to reach equilibrium at a certain  $E_1$  for sufficiently long deposition times ( $t_1$ ).

311 Evidently, while larger  $t_1$  values will favor the attainment of Nernst equilibrium, too long  
312 deposition times will render the technique less useful or even unworkable. The  
313 performance of the AGNES signal as a function of  $t_1$  at various  $E_1$  (ranging from 0.185  
314 to 0.250 V) was evaluated (Figure 3), and the equilibrium (recognized by a plateau) was  
315 attained after 2 to 15 minutes, depending on  $E_1$ ; whereas for an  $E_1$  between 0.250 to 0.230  
316 V the equilibrium was reached within 200 s, it is necessary to wait around 900 s when  
317 using a less positive  $E_1$  of 0.185 V. In the following AGNES experiments, a compromise  
318 between the intensity of the signal and the time needed to reach the equilibrium led to the  
319 choice of using the set  $E_1 = 0.230$  V and  $t_1 = 240$  s.

320 A typical parameter in AGNES is the gain ( $Y$ ), the preconcentration or accumulation  
321 factor, which -following Nernst equation- relates the concentration ratio of reduced to  
322 oxidized species in the case of Hg electrodes. At solid electrodes, the gain can relate the  
323 obtained surface coverage of reduced species with the bulk concentration of oxidized  
324 species [18]. Given the difficulties in finding the standard formal potential,  $E^0$ , at this  
325 type of gold polycrystalline wire electrode, we work here with the operational definition:

$$326 \quad Y = \exp \left[ -\frac{nF}{RT} (E_1 - E_{d,1/2}) \right] \quad (\text{Equation 1})$$

327 where,  $R$  is the gas constant,  $T$  the temperature,  $n$  the number of exchanged electrons,  $F$   
328 the Faraday constant and  $E_{d,1/2}$  is the half wave potential of the SSV waves (0.218 V;  
329 section 3.1). The real gain will differ from the operational one by a multiplying factor,  
330 but this factor cancels out between calibration and measurement, so it does not affect the  
331 determined free metal concentration.

332 The equilibrium signal intensities (that were obtained on the plateau of the various  $E_1$   
333 curves displayed in Figure 3) show a linear behavior (slope =  $2.6 \times 10^{-6}$  with a  $R^2 = 0.988$ ;  
334 Figure 4) with the gain  $Y$ , confirming that the AGNES conditions were attained.

335

336 3.2.2 Variation of the signal with free metal concentration

337 The linearity between the AGNES signal (peak derivative) and the concentration of  $\text{Cu}^{2+}$   
338 was evaluated for the  $E_1$  and  $t_1$  set chosen above ( $E_1 = 0.230$  V and  $t_1 = 240$  s). Moreover,  
339 the range of Cu concentrations that can be used with this potential-time set was defined.  
340 For the chosen experimental setting, a linear behavior was obtained between the DP signal  
341 and the range of free Cu concentrations of  $7.5 \times 10^{-9}$  to  $9.8 \times 10^{-8}$  M ( $y = 19.2 (\pm 0.3) x +$   
342  $7.5 (\pm 1.6) \times 10^{-8}$ ,  $R^2 = 0.999$ ; Figure 5a). In fact, a linear behavior is still obtained up to a  
343 free copper concentration of  $9.8 \times 10^{-7}$  M ( $y = 15.97 (\pm 0.09) x + 2.1 (\pm 0.3) \times 10^{-7}$ ,  $R^2 =$   
344  $0.998$ ), with a deviation from the linearity observed at higher concentrations (Figure 5b).  
345 Obviously, the linearity range can be modified by using different experimental settings.  
346 The limit of detection ( $\text{LOD} = (3.3 \text{SE}_y)/m$ ; where  $\text{SE}_y$  is the standard error for the  $y$   
347 estimate, and  $m$  is the slope) for the  $E_1$  and  $t_1$  set chosen ( $E_1 = 0.230$  V and  $t_1 = 240$  s) is  
348  $1.1 \times 10^{-8}$  M. It was not the focus of this study to reach lower LOD. However, this can  
349 easily be achieved by applying higher gains, although longer deposition times would be  
350 required to attain AGNES conditions (Figures 3 and 4), leading to analysis time between  
351 15 and 30 min per measurement. Another option is the use of smaller diameter electrodes  
352 and/or increasing vibrations to increase the diffusion flux, allowing the achievement of  
353 higher gains with similar deposition times.

354

### 355 3.3. Equilibrium Speciation

356 The possibility to perform AGNES on the VGME was tested by quantifying the  
357 equilibrium speciation of Cu in presence of the two ligands forming labile complexes,  
358 malonic acid (MAL) and iminodiacetic acid (IDA) (Tables 1 and 2, respectively; obtained  
359 by using the set  $E_1 = 0.230$  V and  $t_1 = 240$  s; for the lability calculation see section 3.4).  
360 The free copper concentration at various concentrations of ligands and pH were directly  
361 determined from the calibration curve (Figure 5a) [7]. This concentration can be then used  
362 to calculate the conditional stability constant ( $K$ ) by using the following equation:

$$363 \quad K = \left( \frac{c_{M,T}}{c_{M,free}} - 1 \right) / c_{L,dep} \quad (\text{Equation 2})$$

364 where,  $c_{M,T}$  and  $c_{M,free}$  are the total and free metal concentrations, respectively, and  $c_{L,dep}$   
 365 being the fully-deprotonated ligand concentration available for Cu complexation at each  
 366 specific pH value and ionic strength (computed using Visual Minteq [34]).

367 Both the quantified free Cu concentrations and the calculated log  $K$  values were compared  
 368 with those obtained by Visual Minteq (Tables 1 and 2). As expected, for both systems,  
 369 the free Cu concentrations were found to decrease with an increase of pH, and at fixed  
 370 pH, an increase of the ligand concentration resulted in lower free Cu concentrations. For  
 371 both ligands, the free Cu concentrations (and, consequently, the conditional stability  
 372 constants) determined by AGNES in all conditions of ligand concentrations and pH were  
 373 found identical, within the experimental error, to the values obtained by the equilibrium-  
 374 based computer code.

375 In fact, these results clearly show that AGNES at the VGME can successfully quantify  
 376 free metal concentrations in simple systems at acidic pH and relatively low ionic  
 377 strengths. Despite the quite laborious electrochemical set-up (optimization is underway),  
 378 the data obtained are reproducible (shown by the errors associated with measurements).

379

### 380 *3.4. Comparison between AGNES and SSV*

381 The results obtained by AGNES were also compared to another analytical technique, the  
 382 SSV analysis. The possibility of performing SSV of Cu using the VGME had already  
 383 been shown by Gibbon-Walsh *et al.* [21]. SSV determinations allow the direct  
 384 determination of the conditional stability constant ( $K$ ) of labile systems from the shift in  
 385 the half-wave deposition potentials considering the formation of a reversible complex  
 386 [38]:

$$387 \quad K = \left( \exp \left( - \left( \frac{nF}{RT} \right) \Delta E_{d,1/2} - \ln \left( \frac{s_{ML}^*}{s_M^*} \right) \right) - 1 \right) / c_{L,dep} \quad (\text{Equation 3})$$

388 where,  $\Delta E_{d,1/2}$  is the shift in the half-wave deposition potential between M in absence  
 389 and in presence of the ligand, and  $s_M^*$  and  $s_{ML}^*$  the diffusion limiting values of the stripping  
 390 signal in absence and in presence of the ligand.

391 Therefore, it is possible to directly compare the speciation data of AGNES with that of  
 392 SSV, although the former measures directly the free metal concentration which allows  
 393 calculation of the conditional stability constant  $K$  (equation 2), while for SSV it is the  
 394 other way round (it measures directly  $K$  allowing retrieval of free metal concentration by  
 395 using the same equation 2).

396 An extra information that can be obtained when using SSV (not possible with AGNES)  
 397 is the lability coefficient of complexes, which can be calculated from the ratio between  
 398 the limiting kinetic flux,  $J_{kin}$ , and the limiting diffusive flux,  $J_{dif}$  [35]:

$$399 \frac{J_{kin}}{J_{dif}} = c_{ML} k_d \mu \frac{\delta}{D_M c_{M,T}} \quad (\text{Equation 4})$$

400 where,  $c_{ML}$  is the complex concentration,  $\mu$  is the reaction layer thickness, and  $k_d$  the  
 401 dissociation rate constant. The thickness of the diffusion layer ( $\delta$ ) of the VGME used in  
 402 this experimental set up was determined to be 5  $\mu\text{m}$ , whereas the reaction layer thickness  
 403 is given by:

$$404 \mu = \left( \frac{D_M}{k'_a} \right)^{1/2} \quad (\text{Equation 5})$$

405 where,  $k'_a = k_a c_{L,dep}$  and  $k_a$  is the association rate constant which is generally consistent  
 406 with a mechanism in which the formation of an outersphere complex between the metal  
 407 and the ligand, with an electrostatically determined stability constant ( $K^{os}$ ), is followed  
 408 by a rate-limiting removal of water from the inner coordination sphere of the metal ( $k_{-w}$ ).  
 409 This is commonly known as the Eigen mechanism [36]:

$$410 k_a = k_{-w} K^{os} \quad (\text{Equation 6})$$

411 where,  $k_{-w}$ , which is intrinsic for each metal ion, is  $1.0 \times 10^9 \text{ s}^{-1}$  for Cu [37], and  $K^{os}$  is  
 412 given by:

$$413 \quad K^{os} = \frac{4\pi N_{Av} a^3}{3} \exp(-U^{os}) \quad (\text{Equation 7})$$

414 where,  $N_{Av}$  is the Avogadro number,  $a$  is the charge center-to-center distance of closest  
415 approach between the reagents, and  $U^{os}$  is the electrostatic energy which is determined by  
416 a combination of the primary Coulombic energy between the metal and the ligand, with  
417 the energy for the screening effect due to the electrolyte.

418 The characteristic regimes of both metal complex systems, Cu-MAL and Cu-IDA, were  
419 calculated (Table 3) considering the conditions where more complexation occurs, i.e.,  
420 higher ligand concentration and higher pH (stability constants obtained by Visual Minteq  
421 were used; Tables 1 and 2). The results show that both systems are dynamic since the  
422 rates for the volume reactions are fast on the experimental time scale;  $k_d t, k'_a t \gg 1$  (Table  
423 3). The slightly larger than 1 values for the ratio of the kinetic to the diffusive fluxes  
424 indicate that both systems are still labile under these physicochemical conditions when  
425 using the VGME.

426 Table 1 shows the obtained values by SSV ( $\log K$ , and the free metal concentrations  
427 calculated from the stability constants) for  $1.0 \times 10^{-7}$  M of total Cu in presence of  $1.0 \times 10^{-5}$   
428 M of MAL at pH 4.5, 5.0 and 6.0 and  $I = 0.01$  M. They are in very good agreement with  
429 AGNES, despite at pH 5.0 a slight difference is obtained, although still within the  
430 experimental error. The same good agreement was also obtained for the Cu-IDA system  
431 at pH 4.5 and 5.0 (Table 2). The good correlation between the data supports the SSV  
432 calculation methodology for VGME used to calculate the free metal ion concentration,  
433 however, with the AGNES procedure leading to less error than the corresponding shift in  
434 potential in SSV.

435

#### 436 **4. Conclusions**

437 AGNES was successfully implemented at the VGME allowing for the first time the direct  
438 quantification of free Cu concentrations using a solid electrode, where a linear calibration

439 plot was obtained from  $4.9 \times 10^{-9}$  to  $9.8 \times 10^{-7}$  M of free Cu. The validity of AGNES at the  
440 gold electrode was verified by the trajectories reaching equilibrium values and by the  
441 linear dependency of the applied gain  $Y$ .

442 There are not many techniques that can perform the measurement of free metal ion  
443 concentration at low levels, although this is a key parameter to any speciation study and/or  
444 interpretation of the dynamic speciation data obtained with other electroanalytical  
445 techniques [16]. The AGNES methodology at the VGME could thus provide (after further  
446 developments) a powerful alternative technique for Cu speciation at the low concentration  
447 levels existing in natural waters especially due to: i) the non-toxicity of the working  
448 electrode, and ii) the ability to perform measurements without oxygen removal.  
449 Obviously, further optimization of the electrochemical set-up, which is already under  
450 way, is needed to decrease the detection limit that is reported here (11 nM). Such  
451 optimization consists in, for example, the decrease of the electrode diameter and/or  
452 increase of the vibration frequency to lower lower detection limits, which is required for  
453 applications in natural waters. Further testing of the method (e.g., in the presence of humic  
454 substances, and at wider pH and ionic strength ranges) is under way at solid gold  
455 electrodes, as well as at other material substrates (e.g., Ag and C).

456

#### 457 **Acknowledgment**

458 Funding for this work was provided by (i) Fundação para a Ciência e Tecnologia (FCT,  
459 Portugal): Science 2008 IST-CQE3 “Environmental Chemistry” Assistant Researcher  
460 position to RFD and Project PTDC/AAC-AMB/110595/2009, and (ii) ANR-FCT project  
461 N°12-IS06-0001 - SPECIES: “Mesure in situ de la spéciation des métaux trace”, by ANR  
462 Project NormaRHIZO. JG acknowledges financial support from the Spanish Ministry of  
463 Education and Science (project CTM2013-48967).

464

465  
466  
467  
468  
469  
470  
471  
472  
473  
474  
475  
476  
477  
478  
479  
480

481 **References**

- 482 [1] V.I. Slaveykova, K.J. Wilkinson, Predicting the bioavailability of metals and metal  
483 complexes: critical review of the biotic ligand model, *Environ. Chem.*, 2 (2005) 9-24.
- 484 [2] J. Buffle, Study of complexation properties by voltammetric methods, Ellis Horwood,  
485 Chichester, 1988.
- 486 [3] E.J.M. Temminghoff, A.C.C. Plette, R.van Eck, W.H.van Riemsdijk, Determination  
487 of the chemical speciation of trace metals in aqueous systems by the Wageningen Donnan  
488 membrane technique, *Anal. Chim. Acta*, 417 (2000) 149-157.

- 489 [4] R.F. Domingos, M.F. Benedetti, J.P. Pinheiro, Application of permeation liquid  
490 membrane and scanned stripping chronopotentiometry to metal speciation analysis of  
491 colloidal complexes, *Anal. Chim. Acta*, 589 (2007) 261-268.
- 492 [5] P. Salaun, J. Buffle, Integrated microanalytical system coupling PLM and  
493 voltammetry for trace metal speciation – theory and applications, *Anal. Chem.*, 76 (2004)  
494 31-39.
- 495 [6] I.A.M. Worms, K.J. Wilkinson, Determination of Ni<sup>2+</sup> using an equilibrium ion  
496 exchange technique: important chemical factors and applicability to environmental  
497 samples, *Anal. Chim. Acta*, 616 (2008) 95-102.
- 498 [7] J. Galceran, E. Companys, J. Puy, J. Cecília, J.L. Garcés, AGNES: a new  
499 electroanalytical technique for measuring free metal ion concentration, *J. Electroanal.*  
500 *Chem.*, 566 (2004) 95-109.
- 501 [8] R.F. Domingos, A. Gélabert, S. Carreira, A. Cordeiro, Y. Sivry, M.F. Benedetti,  
502 Metals in the aquatic environment—interactions and implications for the speciation and  
503 bioavailability: a critical overview, *Aquatic Geochem.*, 21 (2014) 231-257.
- 504 [9] M. Pesavento, G. Alberti, R. Biesuz, Analytical methods for determination of free  
505 metal ion concentration, labile species fraction and metal complexation capacity of  
506 environmental waters: A review, *Anal. Chim. Acta*, 631 (2009) 129-141.
- 507 [10] J. Feldmann, P. Salaun, E. Lombi, Critical review perspective: elemental speciation  
508 analysis methods in environmental chemistry - moving towards methodological  
509 integration, *Environ. Chem.*, 6 (2009) 275-289.
- 510 [11] E. Bakker, E. Pretsch, The new wave of ion-selective electrodes, *Anal. Chem.*, 74  
511 (2002) 420A-426A.
- 512 [12] E. Pretsch, The new wave of ion-selective electrodes, *Trends Anal. Chem.*, 26 (2007)  
513 46-51.

- 514 [13] E. Companys, J. Puy, J. Galceran, Humic acid complexation to Zn and Cd  
515 determined with the new electroanalytical technique AGNES, *Environ. Chem.*, 4 (2007)  
516 347-354.
- 517 [14] J. Galceran, C. Huidobro, E. Companys, G. Alberti, AGNES: A technique for  
518 determining the concentration of free metal ions. The case of Zn(II) in coastal  
519 Mediterranean seawater, *Talanta*, 71 (2007) 1795-1803.
- 520 [15] F. Zavarise, E. Companys, J. Galceran, G. Alberti, A. Profumo, Application of the  
521 new electroanalytical technique AGNES for the determination of free Zn concentration  
522 in river water, *Anal. Bioanal. Chem.*, 397 (2010) 389-394.
- 523 [16] R.F. Domingos, C. Huidobro, E. Companys, J. Galceran, J. Puy, J.P. Pinheiro,  
524 Comparison of AGNES (absence of gradients and Nernstian equilibrium stripping) and  
525 SSCP (scanned stripping chronopotentiometry) for trace metal speciation analysis, *J.*  
526 *Electroanal. Chem.*, 617 (2008) 141-148.
- 527 [17] D. Omanovic, C. Garnier, Y. Louis, V. Lenoble, S. Mounier, I. Pizeta, Significance  
528 of data treatment and experimental setup on the determination of copper complexing  
529 parameters by anodic stripping voltammetry, *Anal. Chim. Acta*, 664 (2010) 136-143.
- 530 [18] L.S. Rocha, J. Galceran, J. Puy, J.P. Pinheiro, Determination of the free metal ion  
531 concentration using AGNES implemented with environmentally friendly bismuth film  
532 electrodes, *Anal. Chem.*, 87 (2015) 6071-6078.
- 533 [19] P. Salaun, C.M.G.van den Berg, Voltammetric detection of mercury and copper in  
534 seawater using a gold microwire electrode, *Anal. Chem.*, 78 (2006) 5052-5060.
- 535 [20] C.S. Chapman, C.M.G.van den Berg, Anodic stripping voltammetry using a  
536 vibrating electrode, *Electroanalysis*, 19 (2007) 1347-1355.
- 537 [21] K. Gibbon-Walsh, P. Salaun, C.M.G.van den Berg, Pseudopolarography of copper  
538 complexes in seawater using a vibrating gold microwire electrode, *J. Phys. Chem. A*, 116  
539 (2012) 6609-6620.

- 540 [22] Y. Bonfil, M. Brand, E. Kirowa-Eisner, Determination of mercury and copper in  
541 waste water by anodic-stripping voltammetry at the gold electrode, *Reviews in Anal.*  
542 *Chem.*, 19 (2000) 201-216.
- 543 [23] D. Aguilar, J. Galceran, E. Companys, J. Puy, C. Parat, L. Authier, M. Potin-Gautier,  
544 Non-purged voltammetry explored with AGNES *Phys. Chem. Chem. Phys.*, 15 (2013)  
545 17510-17521.
- 546 [24] L.S. Rocha, E. Companys, J. Galceran, H.M. Carapuça, J.P. Pinheiro, Evaluation of  
547 thin mercury film rotating disk electrode to perform absence of gradients and Nernstian  
548 equilibrium stripping (AGNES) measurements, *Talanta*, 80 (2010) 1881–1887.
- 549 [25] V. Sosa, C. Barceló, N. Serrano, C. Arino, J.M. Dáz-Cruz, M. Esteban, Antimony  
550 film screen-printed carbon electrode for stripping analysis of Cd(II), Pb(II), and Cu(II) in  
551 natural samples *Anal. Chim. Acta*, 855 (2015) 34-40.
- 552 [26] P. Salaun, K.B. Gibbon-Walsh, G.M.S. Alves, H.M.V.M. Soares, C.M.G. van den  
553 Berg, Determination of arsenic and antimony in seawater by voltammetric and  
554 chronopotentiometric stripping using a vibrated gold microwire electrode, *Anal. Chim.*  
555 *Acta*, 746 (2012) 53-62.
- 556 [27] Z. Bi, P. Salaun, C.M.G. van den Berg, The speciation of lead in seawater by  
557 pseudopolarography using a vibrating silver amalgam microwire electrode, *Mar. Chem.*,  
558 151 (2013) 1-12.
- 559 [28] L. Nyholm, G. Wikmark, Microelectrodes for anodic stripping voltammetry prepared  
560 by heat sealing thin fibres or wires in a polypropylene matrix, *Anal. Chim. Acta*, 257  
561 (1992) 7-13.
- 562 [29] K. Gibbon-Walsh, P. Salaun, C.M.G. van den Berg, Determination of manganese and  
563 zinc in coastal waters by anodic stripping voltammetry with a vibrating gold microwire  
564 electrode, *Environ. Chem.*, 8 (2011) 475-484.

- 565 [30] P. Salaun, F. Frézard, Unexpectedly high levels of antimony(III) in the pentavalent  
566 antimonial drug glucantime: insights from a new voltammetric approach, *Anal. Bioanal.*  
567 *Chem.*, 405 (2013) 5201-5214.
- 568 [31] G. Herzog, D.W.M. Arrigan, Determination of trace metals by underpotential  
569 deposition–stripping voltammetry at solid electrodes, *Trends Anal. Chem.*, 24 (2005)  
570 208-217.
- 571 [32] V. Beni, H.V. Newton, D.W.M. Arrigan, M. Hill, W.A. Lane, A. Mathewson,  
572 Voltammetric behaviour at gold electrodes immersed in the BCR sequential extraction  
573 scheme media. Application of underpotential deposition–stripping voltammetry to  
574 determination of copper in soil extracts, *Anal. Chim. Acta*, 502 (2004) 195-206.
- 575 [33] Y. Bonfil, M. Brand, E. Kirowa-Eisner, Determination of sub- $\mu\text{g L}^{-1}$  concentrations  
576 of copper by anodic stripping voltammetry at the gold electrode, *Anal. Chim. Acta*, 387  
577 (1999) 85-95.
- 578 [34] D.S. Brown, J.D. Allison, MINTEQA1. An equilibrium metal speciation model.  
579 User's manual EPA/600/3-87/012, Athens, GA, 1987.
- 580 [35] H.P. van Leeuwen, R.M. Town, J. Buffle, Impact of ligand protonation on Eigen-type  
581 metal complexation kinetics in aqueous systems, *J. Phys. Chem. A*, 111 (2007) 2115-  
582 2121.
- 583 [36] M. Eigen, Fast elementary steps in chemical reaction mechanisms, *Pure Appl.*  
584 *Chem.*, 6 (1963) 97-115.
- 585 [37] D.W. Margerum, G.R. Cayley, D.C. Weatherburn, G.K. Pagenkopf, Kinetics and  
586 mechanisms of complex formation and ligand exchange, in: A.E. Martell (Ed.)  
587 *Coordination chemistry*, American Chemical Society, Washington DC, 1978.
- 588 [38] J.P. Pinheiro, H.P. van Leeuwen, Scanned stripping chronopotentiometry of metal  
589 complexes: lability diagnosis and stability computation, *J. Electroanal. Chem.*, 570  
590 (2004) 69-75.

591 [39] E.M. Khairy, M.M. Shoukry, M.M. Khalil, M.M.A. Mohamed, Metal complexes of  
592 salicylhydroxamic acid: equilibrium studies and synthesis, *Transition Met. Chem.*, 21  
593 (1996) 176-180.

594 [40] J. Bjerrum, *Stability constants*, Chemical society, London, 1958.

595

596 **Table 1** – Free copper concentrations and log  $K$  values obtained from AGNES, SSV and Visual MinteQ for a total copper concentration of  $1.0 \times 10^{-7}$  M  
 597 and different total malonic acid (MAL) concentrations at  $1.0 \times 10^{-1}$  M and various pH values. Deprotonated MAL concentrations ( $c_{\text{MAL,dep}}$ ) were computed  
 598 by using Visual MinteQ. Diffusion coefficients:  $D_{\text{Cu}} = 7.14 \times 10^{-10} \text{ m}^2 \text{ s}^{-1}$ ;  $D_{\text{MAL}} = 8.45 \times 10^{-10} \text{ m}^2 \text{ s}^{-1}$ . AGNES results are the mean and standard deviation,  
 599 whereas for SSV mean values are presented together with minimum and maximum values obtained from the SSV waves (values within square brackets).

pH	$c_{\text{MAL,dep}} / \text{M}$	AGNES		SSV			VisualMinteQ	
		$c_{\text{Cu,free}} / \text{M}$	log $K$	$c_{\text{Cu,free}} / \text{M}$	log $K$	$\Delta E_{\text{d},1/2} / \text{V}$	$c_{\text{Cu,free}} / \text{M}$	log $K$
4.0	$9.99 \times 10^{-6}$	$(9.0 \pm 0.5) \times 10^{-8}$	$4.1 \pm 0.1$	-	-	-	$9.2 \times 10^{-8}$	4.0
4.5	$9.98 \times 10^{-6}$	$(7.6 \pm 0.7) \times 10^{-8}$	$4.5 \pm 0.2$	$7.1 \times 10^{-8}$ [(4.4-8.7) $\times 10^{-8}$ ]	4.8 [4.2-5.1]	-0.002	$8.1 \times 10^{-8}$	4.4
5.0	$9.96 \times 10^{-6}$	$(6.12 \pm 0.06) \times 10^{-8}$	$4.80 \pm 0.01$	$7.5 \times 10^{-8}$ [(5.4-9.9) $\times 10^{-8}$ ]	5.2 [3.4-5.6]	-0.014	$6.2 \times 10^{-8}$	4.8
5.5	$9.94 \times 10^{-6}$	$(4.24 \pm 0.08) \times 10^{-8}$	$5.14 \pm 0.01$	-	-	-	$4.4 \times 10^{-8}$	5.1
6.0	$9.93 \times 10^{-6}$	$(3.2 \pm 0.2) \times 10^{-8}$	$5.34 \pm 0.04$	$3.3 \times 10^{-8}$ [(2.6-4.3) $\times 10^{-8}$ ]	5.4 [5.3-5.6]	-0.020	$3.3 \times 10^{-8}$	5.3
4.0	$1.00 \times 10^{-4}$	$(5.5 \pm 0.3) \times 10^{-8}$	$3.91 \pm 0.05$		-	-	$5.8 \times 10^{-8}$	3.9

4.5	$9.99 \times 10^{-5}$	$(3.5 \pm 0.4) \times 10^{-8}$	$4.27 \pm 0.08$		-	-	$3.1 \times 10^{-8}$	4.3
5.0	$9.99 \times 10^{-5}$	$(1.5 \pm 0.2) \times 10^{-8}$	$4.74 \pm 0.08$		-	-	$1.4 \times 10^{-8}$	4.8

600

601

602

603

604

605

606

607

608

609

610

611

612 **Table 2** – Free copper concentrations and log  $K$  values obtained by AGNES, SSV and Visual MinteQ for a total copper concentration of  $1.0 \times 10^{-7}$  M  
 613 and different total iminodiacetic acid (IDA) concentrations at  $I$  0.01 M and various pH values. Deprotonated IDA concentrations ( $c_{\text{IDA,dep}}$ ) were  
 614 computed by using VisualMinteQ; IDA constants [39, 40] were added to the database (protonation constants: 2.98 and 9.89; formation constant of Cu-  
 615 IDA: 11.21). Diffusion coefficients:  $D_{\text{Cu}} = 7.14 \times 10^{-10} \text{ m}^2 \text{ s}^{-1}$ ;  $D_{\text{IDA}} = 7.19 \times 10^{-10} \text{ m}^2 \text{ s}^{-1}$ . AGNES results are the mean and standard deviation, whereas  
 616 for SSV mean values are presented together with minimum and maximum values obtained from the SSV waves (values within square brackets).

		AGNES		SSV			VisualMinteQ	
pH	$c_{\text{IDA,dep}} / \text{M}$	$c_{\text{Cu,free}} / \text{M}$	log $K$	$c_{\text{Cu,free}} / \text{M}$	log $K$	$\Delta E_{\text{d},1/2} / \text{V}$	$c_{\text{Cu,free}} / \text{M}$	log $K$
4.0	$9.98 \times 10^{-7}$	$(9.27 \pm 0.03) \times 10^{-8}$	$4.90 \pm 0.02$	-	-	-	$9.6 \times 10^{-8}$	4.7
4.5	$9.92 \times 10^{-7}$	$(8.70 \pm 0.09) \times 10^{-8}$	$5.18 \pm 0.04$	-	-	-	$9.0 \times 10^{-8}$	5.0
5.0	$9.79 \times 10^{-7}$	$(7.56 \pm 0.08) \times 10^{-8}$	$5.52 \pm 0.02$	-	-	-	$7.7 \times 10^{-8}$	5.5
5.5	$9.55 \times 10^{-7}$	$(5.19 \pm 0.04) \times 10^{-8}$	$5.987 \pm 0.006$	-	-	-	$5.4 \times 10^{-8}$	6.0
4.0	$9.98 \times 10^{-6}$	$(7.4 \pm 0.3) \times 10^{-8}$	$4.55 \pm 0.07$	-	-	-	$7.8 \times 10^{-8}$	4.4
4.5	$9.95 \times 10^{-6}$	$(5.2 \pm 0.2) \times 10^{-8}$	$4.97 \pm 0.04$	$5.3 \times 10^{-8}$ [(3.4-9.4) $\times 10^{-8}$ ]	4.9 [3.8-5.3]	-0.0037	$5.3 \times 10^{-8}$	4.9
5.0	$9.93 \times 10^{-6}$	$(2.6 \pm 0.1) \times 10^{-8}$	$5.46 \pm 0.02$	$2.8 \times 10^{-8}$	5.4 [5.2-5.6]	-0.0059	$2.7 \times 10^{-8}$	5.4

				$[(2.1-3.9) \times 10^{-8}]$				
--	--	--	--	------------------------------	--	--	--	--

617

618

619

620

621

622

623

624

625

626

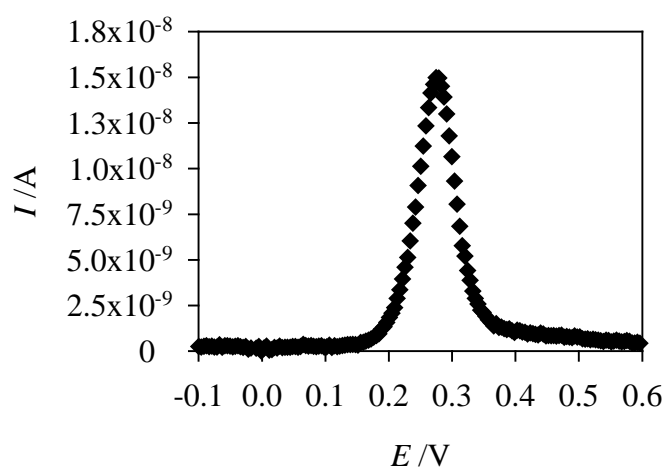
627

628

629 **Table 3** – Characteristic regimes of the metal complex systems. Cu-MAL: total copper  
630 concentration of  $1.0 \times 10^{-7}$  M in presence of  $1.0 \times 10^{-4}$  M of malonic acid at  $I$  0.01 M and  
631 pH 5.0. Cu-IDA: total copper concentration of  $1.0 \times 10^{-7}$  M in presence of  $1.0 \times 10^{-5}$  M of  
632 iminodiacetic acid at  $I$  0.01 M and pH 5.0. The experimental time scale is given by  $t =$   
633  $\delta^2/D_M = 0.035$  s. Other parameters:  $k_{-w} = 1.0 \times 10^9$  s $^{-1}$ ,  $K^{os} = 4.4 \times 10^1$  M $^{-1}$ ,  $U^{os} = -4.9$ ,  $D_M$   
634  $= 7.14 \times 10^{-10}$  m $^2$  s $^{-1}$ ,  $K_{Cu-MAL, VisualMinteq} = 4.8$ ,  $K_{Cu-IDA, VisualMinteq} = 5.4$ .

System	$k'_a t$	$k_d t$	$J_{kin}/J_{dif}$
Cu-MAL	$1.5 \times 10^5$	$2.6 \times 10^4$	56
Cu-IDA	$1.5 \times 10^4$	$5.6 \times 10^3$	33

635



636

637 **Figure 1** – Current as a function of potential for a total copper concentration of  $1.0 \times 10^{-7}$   
638 M at pH 4 and  $I$  0.01 M (adjusted with  $\text{NaNO}_3$ ) obtained by DPASV after subtraction of  
639 the background scan ( $E_d = 0.230$  V,  $t_d = 240$  s).

640

641

642

643

644

645

646

647

648

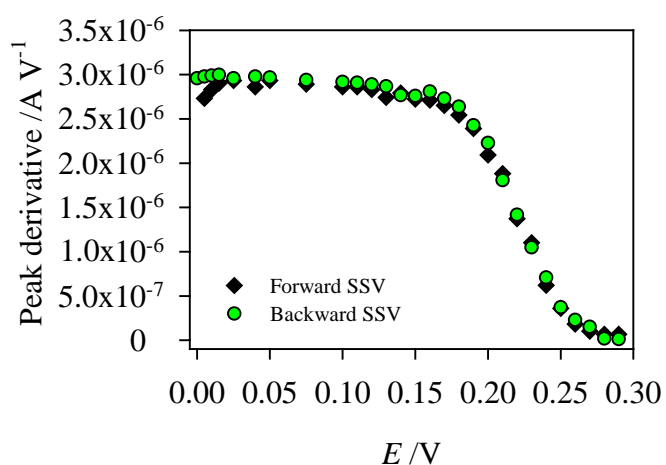
649

650

651

652

653



654

655 **Figure 2** – Forward (◆) and backward (●) SSV of  $1.0 \times 10^{-7}$  M of total Cu at pH 4.0 and656  $I 0.01$  M. Other parameters:  $E_d = 0.000$  to  $0.300$  V and  $t_d = 30$  s.

657

658

659

660

661

662

663

664

665

666

667

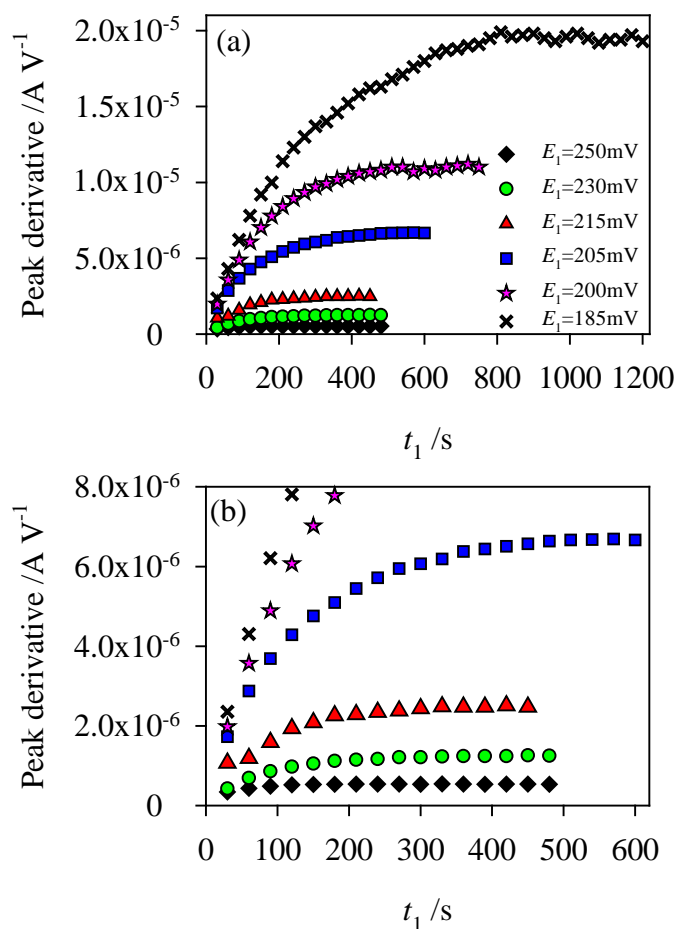
668

669

670

671

672



673

674 **Figure 3** – Peak derivative as a function of deposition time ( $t_1$ ) for a total copper  
 675 concentration of  $1.0 \times 10^{-7}$  M at pH 4.0 and  $I$  0.01 M, and for a range of deposition  
 676 potentials ( $E_1 = 0.185$  to  $0.250$  V). Panel (b) is a zoom of graph in panel (a). The range of  
 677 deposition potentials used was: 250 (◆), 230 (●), 215 (▲), 205 (■), 200 (★), and 185  
 678 (✕) mV.

679

680

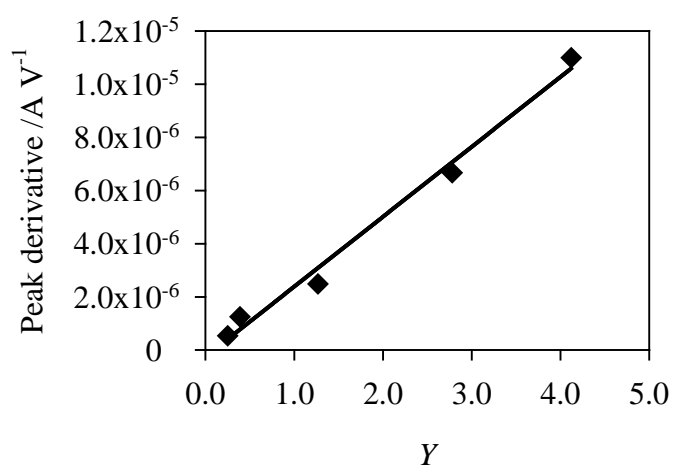
681

682

683

684

685



686

687 **Figure 4** – DP analytical signal after attainment of equilibrium as a function of the gain  
688 for a total copper concentration of  $1.0 \times 10^{-7}$  M at pH 4.0 and  $I$  0.01 M, and for a range of  
689 deposition potentials (0.200 to 0.250 V) and sufficiently long deposition times (240 to  
690 750 s).

691

692

693

694

695

696

697

698

699

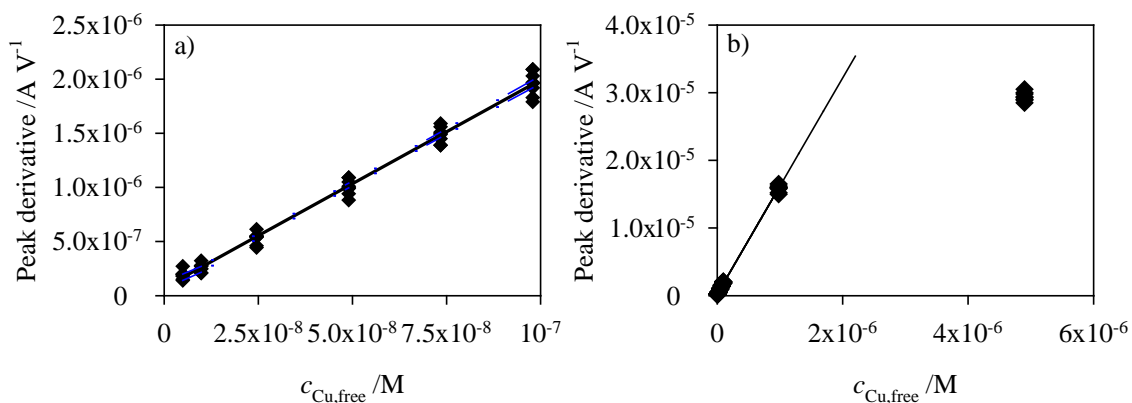
700

701

702

703

704



705

706 **Figure 5** – Peak derivative as a function of free copper concentration at pH 4.0 and  $I$  0.01  
707 M;  $c_{\text{Cu,free}}$ : a)  $4.9 \times 10^{-9}$  to  $9.8 \times 10^{-8}$  M, and b)  $4.9 \times 10^{-9}$  to  $4.9 \times 10^{-6}$  M. The data points are  
708 representative of 8 replicates performed in different days, the solid line represents the  
709 average and the blue long dash lines represent a 95 % confidence level of the root mean  
710 square error. Other parameters:  $E_1 = 0.230$  V,  $t_1 = 240$  s.

711